Pseudorandom Functional BIST for Linear and Nonlinear MEMS

A. Dhayni, S. Mir, L. Rufer, and A. Bounceur
TIMA Laboratory
Grenoble, France
{achraf.dhayni,salvador.mir,libor.rufer,ahcene.bounceur}@imag.fr

Abstract

Pseudorandom test techniques are widely used for measuring the impulse response (IR) for linear devices and Volterra kernels for nonlinear devices, especially in the acoustics domain. This paper studies the application of pseudorandom functional test techniques to linear and nonlinear MEMS Built-In-Self-Test (BIST). We will first present the classical pseudorandom BIST technique for Linear Time Invariant (LTI) systems which is based on the evaluation of the IR of the Device Under Test (DUT) stimulated by a Maximal Length Sequence (MLS). Then we will introduce a new type of pseudorandom stimuli called the Inverse-Repeat Sequence (IRS) that proves better immunity to noise and distortion than MLS. Next, we will illustrate the application of these techniques for weakly nonlinear, purely nonlinear and strongly nonlinear devices.

1. Introduction

Functional testing of analogue circuits is almost always preferred to structural testing approaches largely used for digital circuits. There are several reasons for this. A structural test can fail a circuit for an element value being out of its interval of tolerance, even if it does not cause a performance to fail a specification. This kind of test errors can significantly reduce yield and can only be avoided by functional testing. Another reason is the complexity of fault modeling and fault list prediction in the presence of infinite combinations of parametric defects that can cause faults. For CMOS VLSI circuits, the primary functional elements are transistors (PMOS and NMOS) and their interconnections (metal, polysilicon or diffusion layers). From a simulation point of view, some faults are fortunately much more probable than others. As a result, it has been shown that the infinite combination of parametric faults can in some cases be truncated to simplify fault simulation and fault list prediction necessary for parametric structural testing [1].

For MEMS, only functional testing is today considered during production. Structural testing for MEMS is also being investigated, but it may be even harder to apply than for electrical analog circuits. This is because the large variety of primary functional elements (e.g. cantilever beams, moving and/or twisting plates, gears, hinges, etc.).

Several authors have considered self-test techniques for MEMS, in particular for accelerometers [2,3,4]. Dedicated mechanical beams are used to generate an electrostatic force that mimics an external acceleration. The same idea was introduced in commercial accelerometers [5]. Alternative methods of self-test stimuli generation have been considered (e.g. electrothermal stimuli [3,6] and electromechanical [7]). All these approaches apply electrical test pulses to stimulate the device. The transducer response is next analyzed off-chip. The work in [2] suggests computer-controlled verification and calibration when a Digital Signal Processor (DSP) is available on chip. The differential BIST presented in [8] addresses some limitations of previous self-test approaches but is only applicable for structural testing of differential sensors. A similar approach is presented in [9]. In both cases, functional testing is not considered.

For the above mentioned reasons, we will consider in this paper functional testing of MEMS. Since most MEMS can be stimulated using electrical test pulses, the pseudorandom approach is especially well suited. Pseudorandom testing of mixed-signal circuits has been introduced in [10]. An earlier work based on pulse-like excitation and subsequent analysis of the transient response of a mixed signal circuit is presented in [11]. However, none of these works includes a study on the circuit implementation of the BIST technique and a comparison between different IR measurement methods taking into consideration noise and nonlinear distortions. In addition, none of these previous works consider the extension to nonlinear systems. This paper will address all these issues for the case of MEMS devices.

The IR of a LTI DUT provides enough information about the system functional evaluation. Several techniques have been proposed to measure the IR response using signal processing. These can be classified into four classes:

- White Noise technique, in which the stimulus is a white noise and the IR is calculated by finding the DUT input/output crosscorrelation.
- Time-delay Spectrometry (TDS) [16], like the logarithmic sine sweep [17] and the linear sine sweep. In the linear sine sweep the IR is usually calculated by the inverse Fourier transform of the output signal. In the logarithmic sine sweep it is usually calculated by the deconvolution of the output with respect to the input using an inverse filter.
- Pulse Excitation (PE) technique, in which a single short duration pulse excitation signal is applied and the IR is directly obtained at the output of the DUT.
- Pseudo Random (PR) technique, in which the test stimulus is a pseudo random white noise (like the MLS and the IRS) and the IR is found using the input/output crosscorrelation.

Among the above four techniques the PE and the PR are the most suitable for BIST implementation. In PR, the test signal (MLS or IRS) generator and the input/output correlation can be simply implemented as shown in Section 2. However, this is not the case of the white noise technique where the input/output crosscorrelation needs hardware to carry out multiplication operations, and is thus less suitable for BIST. TDS techniques require also extensive hardware for the sine

3-9810801-0-6/DATE06 © 2006 EDAA

sweep generator, for the inverse Fourier transform calculator [16] or for the inverse filter needed to perform the deconvolution of the output signal with respect to the input [17].

In this paper, only the most suitable IR measurement techniques, PE and PR, are applied to a commercial MEMS accelerometer in the presence of weak nonlinearities. They are then evaluated according to their immunity to nonlinear and noise distortions. The pseudorandom test methods will prove high suitability for BIST implementation, and good immunity to noise and nonlinear distortion. This is in particular true for the IRS technique that is used here for the first time in analog testing.

Next, the pseudorandom method is applied for the case of pure nonlinear systems. Here, a microbeam with electro-thermal excitation and piezoresistive detection is used as a case study. Finally, the pseudorandom method will be generalized for testing nonlinear systems using a multilevel pseudorandom stimulus. For nonlinear systems, the pseudorandom method is used for the extraction of the Volterra kernel coefficients [12], typically used to model nonlinear systems, although this will require in general an on chip DSP.

2. Overview of the pseudorandom test method

In [13] the authors have presented a MEMS pseudorandom test technique. The architecture of the BIST approach is shown in Figure 1. An *m*-order LFSR (Linear Feedback Shift Register) generates a periodic two-level deterministic MLS stimulus of length $L = 2^m - 1$. The analog output of the DUT is then digitized via a self testable 16-bit ADC [20], and correlated with the MLS stimulus to evaluate some IR samples. In [14], the authors map test specifications from the transfer function space to the impulse response space using Monte Carlo simulations, providing a tolerance range in this second space. A sensitivity analysis is performed to choose the IR samples with highest sensitivity to faults, thus, forming the signature that permits the best fault coverage. During testing, the signature from the selected samples is compared with the expected tolerance range in the comparator block of Figure 1.

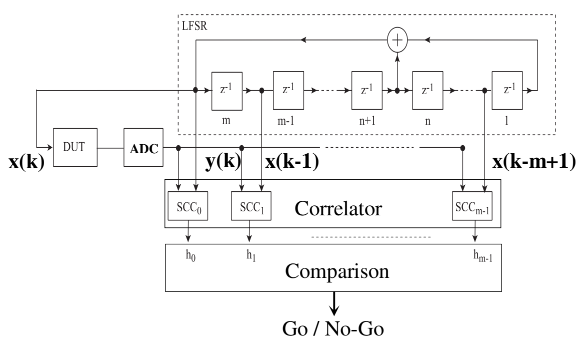

Figure 1. Block diagram of the test approach

The discrete output is y(k)=x(k)*h(k). The input/output cross-correlation ϕ_{xy} can be written in terms of the convolution.

$$\begin{aligned}\phi_{xy}(k) &= y(k) * x(-k) \\ &= h(k) * \left(x(k) * x(-k)\right) \\ &= h(k) * \phi_{xx}(k) \\ &\cong h(k) \qquad \text{if} : \phi_{xx}(k) \cong \delta(k)\end{aligned} \tag{1}$$

An important property of an MLS is that its autocorrelation function ϕ_{xx} is, except for a small DC error, an impulse that can be represented by the Dirac delta function. Thus, as shown in Equation 1, crosscorrelating the system input and output sequences gives the IR. The cross-correlation is defined by:

$$\phi_{xy} = \frac{1}{L} \sum_{j=0}^{L-1} x(j-k)\,y(j) \tag{2}$$

Since the elements of x(k) are all ±1, only additions and subtractions are required to perform the multiplication in the above correlation function. To obtain the k^{th} component h(k) of the IR, the circuit of Figure 2 implements Equation 2.

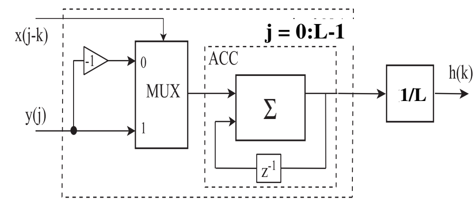

Figure 2. Simplified Correlation Cell (SCC)

Each sample of the output sequence y(j) is multiplied by 1 or –1 by means of the multiplexer unit (MUX) controlled by the input sequence x(j-k), and the result is added L times to the sum stored in the accumulator. The value obtained at the end of the calculation loop is divided by L using a shifter. The output is the k^{th} sample h(k) of the IR of the DUT, knowing that k is equal to the number of delay samples of the MLS stimulus x (j-k) at the input of the SCC.

3. Weakly nonlinear systems

There are always some sources of nonlinear distortion in ideally linear systems. The term "weakly nonlinear system" is used in this context. The sources of nonlinear distortion can be due to MEMS non-idealities, to harmonic and intermodulation distortions of the ADC, and to measurement distortions of any analog signal conditioning circuits. Different IR measurement techniques are more or less affected by distortion depending on the test signal and signal processing used to calculate the IR.

Any weakly nonlinear system can be modeled by the nonlinear model used by [19] and shown in Figure 3.

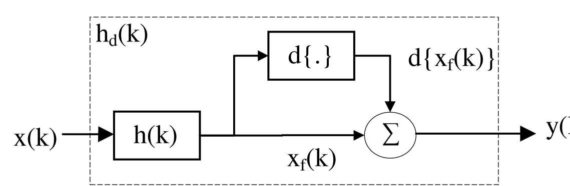

Figure 3. Nonlinear system modeling

A memoryless *r*–order nonlinearity d{.} can be written as:

$$d\left\{x_f(k)\right\} = A_d\left[x_f(k)\right]^r \tag{3}$$

where A_d sets the amplitude of the nonlinearity.

The distortion immunity I_d of the impulse measurement can be derived as the ratio of the linear IR energy to the nonlinear error energy [19] as follows:

$$I_d = 10\log_{10}\left[\frac{\sum_{k=0}^{L-1} h^2(k)}{\sum_{K=0}^{L-1} e_{nl}^2(k)}\right] \tag{4}$$

Distortion immunity is an important performance parameter for evaluating an IR measurement technique. But measurement environments suffer both nonlinear distortion and noise. So immunity to noise must be considered as well. In Section 3.2 the distortion and noise immunities for each method are evaluated. First, the pseudorandom IRS technique is introduced.

3.1. Inverse-Repeat Sequence technique

Consider a periodic binary signal x(k) suitable for impulse response measurement, where the second half of the sequence is the exact inverse of the first half, that is:

$$x(k+L) = -x(k) \tag{5}$$

The period of 2L of such a sequence will always contain an even number of samples. It is proved in [19] that all even-order autocorrelations (r even) are exactly zero. Such a sequence therefore possesses complete immunity to even-order nonlinearity after cross correlation. Due to the anti symmetry in x(k) the first order autocorrelation will also possess anti symmetry about L, that is, $\phi_1(k) = -\phi_1(n+L)$. A signal that satisfies these conditions is the so-called Inverse-Repeat Sequence (IRS), obtained from two periods of MLS s(k) such that the next period is inverted.

$$\begin{aligned} x(k) &= s(k) \quad n \text{ even}, 0 \le n < 2L \\ &= -s(k) \quad n \text{ odd}, 0 \le n < 2L \end{aligned} \tag{6}$$

where L is the period of the generating MLS (note that the IRS period is 2L which doubles the test time). The first-order autocorrelation of an IRS ϕ_{IRS1} is related to the corresponding signal for the generating MLS by the following expression:

$$\begin{aligned} \phi_{IRS}(k) &= \frac{1}{2(L+1)} \sum_{n=0}^{2l-1} x(k)x(k+n) \\ &= \phi_{MLS}(k), \quad k \text{ even} \\ &= -\phi_{MLS}(k), \quad k \text{ odd} \\ &= \delta(k) - \frac{(-1)^k}{L+1} - \delta(k-L), \qquad 0 \le k < 2L \end{aligned} \tag{7}$$

clearly showing anti-symmetry about L.

By exciting a linear system with an IRS, it is possible to obtain the impulse response of the system like in the case of an MLS excitation. The IRS is generated using an LFSR, and since it is a 2-level sequence the input/output crosscorrelation can be done using the SCC blocks. So the same BIST as the MLS can be used for the IRS technique.

3.2. Comparison between PE and PR techniques

For each of the PE, MLS and IRS techniques we have used the model of Figure 3 to calculate the nonlinear error signal $e_{nl}(k)$ according to the equations defined in [19]. Once $e_{nl}(k)$ is found, the distortion immunity I_d can be calculated. Table 1 shows distortion immunities of each of the three techniques for distortion orders from 2 to 5. The amplitude of the excitation signal is 20 dBm and that of distortion is A_d = -20dBm. The commercial MEMS accelerometer ADXL105 from Analog Devices is taken as a DUT.

Table 1 shows that IRS has a very high immunity advantage over MLS (235.6 dB at the second-order nonlinearity and 79.3 dB at the fourth-order nonlinearity). However only approximately 3 dB of immunity advantage can be offered by the IRS for the case of odd-order nonlinearity. So, the IRS appears more interesting when testing a DUT with even-order nonlinearities. However, in the presence of just odd-order nonlinearity, choosing the MLS is better because it is simpler, and the 3 dB of immunity advantage offered by the IRS can be compensated by a single averaging of the output sequence in the case of an MLS input. The presence of only odd-order nonlinearities is typical of the systems that have odd symmetry, such as "differential" or "balanced" systems.

Table 1. Evaluation of PE, MLS and IRS test techniques

Distortion order r	Distortion immunity (dB)			Noise and distortion immunity advantage of	
	I_d(PE)	I_d(MLS)	I_d(IRS)	MLS over PE	IRS over MLS
2	41.4	16.1	248.7	7.7	235.6
3	63.9	22.1	23.3	12.1	3.6
4	86.4	22.6	251.7	11.84	79.3
5	109.7	25.1	28.1	11.9	3.7

4. Purely nonlinear systems

In general, purely nonlinear systems can be modeled by the Hammerstein model shown in Figure 4. The term "purely nonlinear" stands for the absence of any linear behavior. This is caused by the nonlinear function at the input of the dynamic linear block.

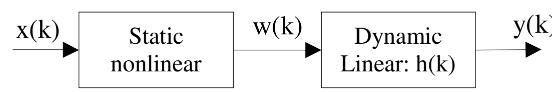

Figure 4. Hammerstein model

As a case study of a purely nonlinear system, a cantilever with electrothermal stimulation and piezoresistive detection has been considered. Figure 5 shows the image of a chip containing 3 microbeams fabricated in a 0.8 µm CMOS bulk micromachining technology. The surface of each cantilever is covered with heating resistors made of polysilicon. The heating of the cantilever causes it to bend and the actual deflection is measured by means of piezoresistors placed at the anchor side of the cantilevers. For each cantilever, a Wheatstone bridge is used for measurement.

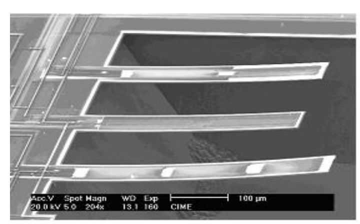

Figure 5. Image of a fabricated microstructure

The average temperature T_m of the MEMS structure depends on the injected thermal power P_{th} that is a function of the voltage V_i applied on the heating resistance R_h according to:

$$P_{th} = \frac{V_i^2}{R_h} \tag{8}$$

In this application the presence of an electrothermal coupling makes the circuit purely nonlinear. The nonlinearity is thus static and of 2^{nd} order. According to the Hammerstein model, the dynamic linear part is the linear IR of the suspended microbeam, and the static nonlinear part corresponds to the squaring function induced by electrothermal excitation. The pseudorandom test introduced in Section 2 is not applicable for a purely 2^{nd} order nonlinear system. For example, if the microbeam is stimulated by an MLS with 1 and -1 levels, $MLS_{(1,-1)}$, the sequence will be squared by the electrothermal excitation resulting in a DC signal at the input of the linear part. Of course, a DC signal is not sufficient to stimulate a linear system with memory.

To avoid this effect, a modified binary MLS with 0 and 1 levels, $MLS_{(0,1)}$, can be used. Its autocorrelation can be deduced from that of $MLS_{(1,-1)}$ according to the following:

$$MLS_{(0,1)}(k) = (MLS_{(1,-1)}(k)+1)/2 \quad \text{for} \quad k=[0, L-1]$$
$$\Rightarrow \phi_{(0,1)}(k) = \frac{\phi_{(1,-1)}(k)}{4} + \frac{L-k}{4L} \approx \frac{\delta(k)}{4} + \frac{L-k}{4L} \tag{9}$$

For x = $MLS_{(0,1)}$ and k = [0, L-1], substituting Equation 9 in Equation 1 leads to:

$$\phi_{xy}(k) = h(k) * \left[\frac{\delta(k)}{4} + \frac{L-k}{4L}\right]$$
$$= \frac{h(k)}{4} + \frac{1}{4}\sum_{i=0}^{k} h(i) - \frac{1}{4L}\sum_{i=0}^{k} h(i)(k-i) \tag{10}$$

Equation 10 shows how h(k) can be extracted out of $\phi_{xy}(k)$ when an $MLS_{(0,1)}$ is used. This also means that $\phi_{xy}(k)$ and h(k) are highly correlated which permits to form the signature in the crosscorrelation space rather than the impulse response space.

This modification can be generalized. According to the Hammerstein model in Figure 4, once x(k) is chosen such that x(k) = w(k), the crosscorrelation of x(k) and y(k) can be derived as function of h(k) as in Equation 10.

In the case of the case-study microbeam, h(k) is the IR of the linear part of the model, which corresponds to the microbeam without considering an electrothermal excitation. Figure 6 shows the calculated impulse response h(k) of the microbeam using Equation 10. Notice the resemblance between h(k) and the diagonal of the 2^{nd} Volterra kernel in Figure 7. Volterra kernels are functions used to model nonlinear systems as discussed in Section 5.

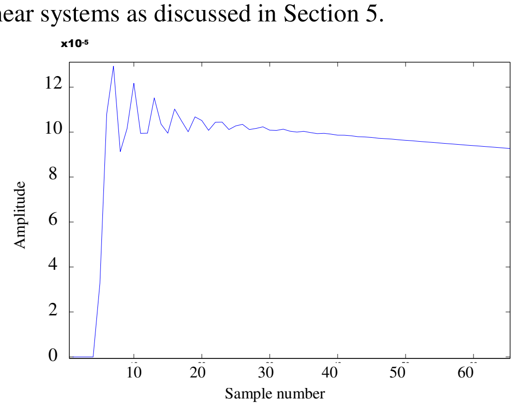

Figure 6. (a) IR of the microbeam

Therefore, for MEMS that can be modeled by the Hammerstein model, there is no need of sophisticated nonlinear modeling since the same results can be obtained with a simple modification of the test signal in the proposed BIST.

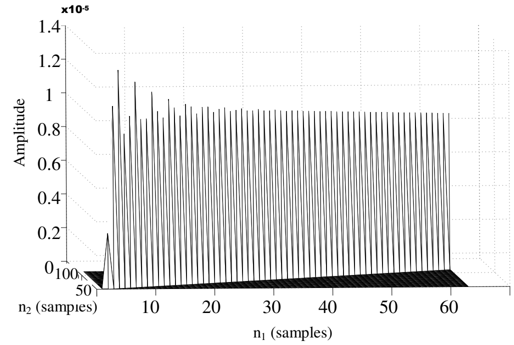

Figure 7. 2^{nd} Volterra kernels of the microbeam

According to [14], a signature of only five samples of the IR of the microbeam is necessary to be compared with the tolerance range in the IR space. The choice of this signature was done according to the sensitivity analysis explained in [14]. For the case of the microbeam, Table 2 shows test quality parameters corresponding to different LFSR lengths and ADC bit precision in the BIST of Figure 1. The values in bold correspond to the case of unacceptable test quality parameters (test escapes > 100 ppm).

Table 2. Test quality results

LFSR length	Bit precision (bits)	Probability of false acceptance	Probability of false rejection	% of test escapes
14	16	0.00005	0.00183	0.000967
	15	0.001	0.00284	0.002
	14	0.0041	0.0098	0.00827
	13	0.1565	0.0095	**0.32**
13	16	0.00326	0.00567	0.00326
	15	0.016	0.009	**0.016**
	14	0.089	0.0104	**0.09**
12	**16**	0.01	0.0257	**0.0175**

According to Table 2 more than 12 bits in the LFSR are necessary to carry out the test with a small percentage of test escapes. Increasing the length of the LFSR results in a lower percentage of test escapes at the expense of longer testing times. It is also possible to derive the minimum number of ADC bits for different lengths of the LFSR. For a 12-bit LFSR, more than 16 bits would be required. For a 13-bit LFSR, the minimum number of ADC bits is 16. As a compromise between complexity, test quality and test time, a 14-bit LFSR with 15 precision bits has been chosen for our design. Notice that the number of precision bits in the signature analyzer must be lower than that of the self testable ADC [20].

5. Strongly nonlinear systems

We consider next nonlinear systems that cannot be modeled according to the simple Hammerstein model used for purely nonlinear systems. In this work we make use of the Volterra modeling technique to test strongly nonlinear devices. Any time-invariant nonlinear system with fading memory can be approximated by a finite Volterra series given by:

$$y(k) = h_o + \sum_{r=1}^{N}\sum_{m_1=0}^{M-1}\cdots\sum_{m_r=0}^{M-1} h_r(m_1,\ldots,m_r)\prod_{j=1}^{r} x(k-m_j) \tag{11}$$

where x and y are respectively the input and output of the system, N is the nonlinearity order, M is the memory of the system, and $h_r(m_1,\ldots,m_r)$ represents a coefficient of the r^{th} order Volterra kernel h_r. The kernel h_r carries information about the *r*-order nonlinear behavior of the system.

The physical meaning of Volterra kernels are illustrated with the block models shown in Figure 8. Figure 9 shows the 1st and 2nd kernels of each of these models, calculated by the algorithm that is explained below.

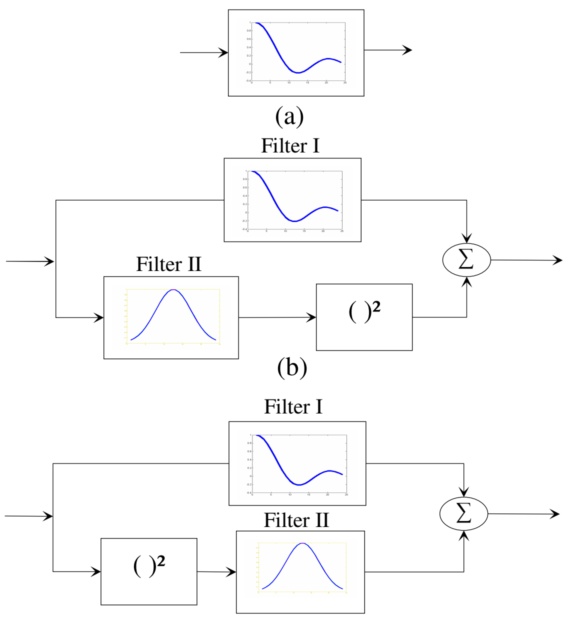

Figure 8. (a) linear system, (b) & (c) 2nd order nonlinear systems

The first two kernels of the linear system in Figure 8(a) are shown in Figure 9(a) and Figure 9(b) respectively. Notice how the 1st kernel represents the linear impulse response and the 2nd kernel is equal to zero since the system is linear. The first two kernels of the nonlinear system of Figure 8(b) are shown in Figure 9(a) and Figure 9(c) where the 2nd kernel is not equal to zero anymore. The 1st kernel is always the same because the linear part of the systems in Figure 8(a) and Figure 8(b) is the same. Similarly, the system of Figure 8(c) has the same 1st kernel and the 2nd kernel is shown in Figure 9(d).

After finding the Volterra kernels, it is possible to extract design properties out of these kernels and prove that they correspond to the functional system. For example, the 1st kernel in Figure 9(a) is nothing but the impulse response of the FIR Filter I which plays the role of the linear part in the systems of Figure 8. This proves the correctness of the 1st kernel. The nonlinearity of the system in Figure 8(c) is represented by squaring each input sample. Thus, there is no multiplication between different input samples at different delays, which means that all the 2nd kernel coefficients at $n_1 \neq n_2$ are zero. That is why Figure 9(d) has values only through the diagonal $(n_1 = n_2)$. Moreover, the values through the diagonal correspond to the impulse response of the FIR Filter II since it is in cascade with the squaring function.

The aim of the test approach is to calculate the kernel coefficients of a nonlinear DUT and to compare them with the typical values to test the device. Existing methods for the identification of Volterra kernels have proved computationally burdensome. In [12] the authors have proposed an efficient method to determine the Volterra kernels, where they make use of the general Wiener model shown in Figure 10.

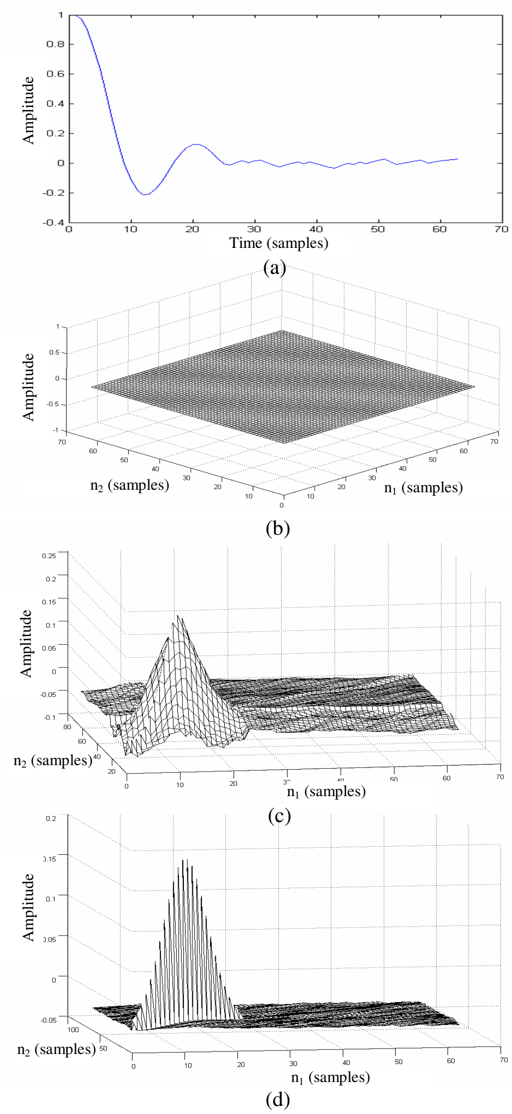

Figure 9. Volterra kernels of the systems in Figure 8. (a) 1st kernel for all systems, (b), (c) and (d) 2nd kernels for the systems in Figure 8(a), 10(b) and 10(c)

According to this method, the system is stimulated by a multilevel MLS (Figure 11) to extract the Wiener coefficients from the values of the sampled output response. The advantage of this method is that the multilevel MLS stimulus can be easily generated on-chip. The Volterra kernels are then obtained from the Wiener model using an on chip calculation [12] by means of a DSP.

It can be proved that applying the pseudorandom test method results in:

$$\Phi_{xy}(k) = \sum_{i=0}^{L-1} h_1(i)\phi_1(k-i) + \sum_{i=0}^{L-1}\sum_{j=0}^{L-1} h_2(i,j)\phi_2(k-i,k-j)$$
$$+ \sum_{i=0}^{L-1}\sum_{j=0}^{L-1}\sum_{m=0}^{L-1} h_3(i,j,m)\phi_3(k-i,k-j,k-m) + \ldots \qquad (12)$$

where each term is an *r*-dimensional convolution of a Volterra kernel $h_r(k_1, k_2 .... k_r)$ with the r-dimensional autocorrelation function of the input sequence ϕ_r $(k_1, k_2 .... k_r)$. The first term, $\sum_{i=0}^{L-1} h_1(i)\phi_1(k-i)$, equals $h_1(k)$ for the case of an MLS, which means that $\Phi_{xy}(k)$ is directly related to $h_1(k)$, the linear behavior of the system. Physically, when a fault exists it always harms both the linear behavior $h_1(k)$ which is highly correlated with $\Phi_{xy}(k)$, and the nonlinear one. Therefore, the presence of a fault will have an influence on the value of $\Phi_{xy}(k)$ which means that the pseudorandom test method is valid for nonlinear systems.

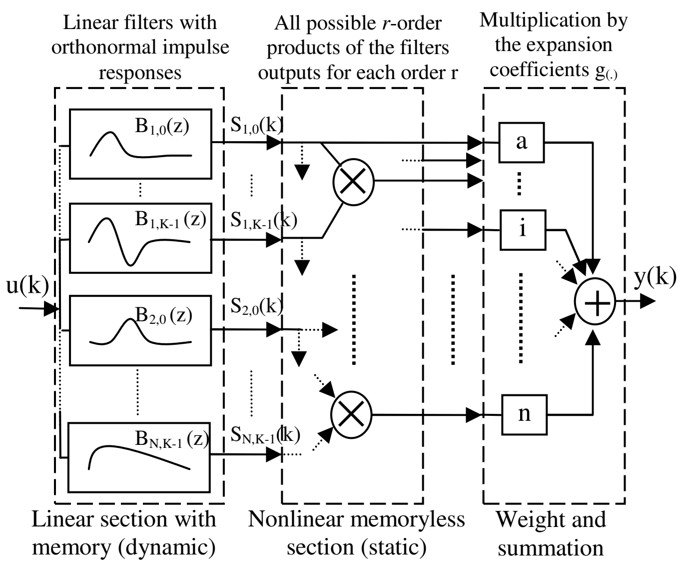

Figure 10. Wiener model with orthonormal basis

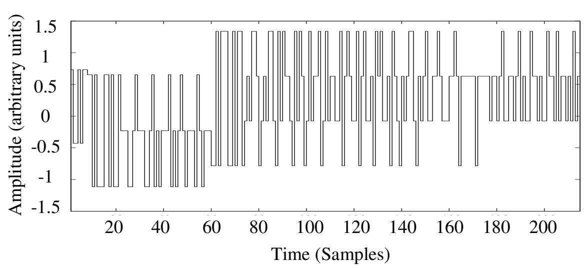

Figure 11. Multilevel MLS stimulus

An illustration of the use of multilevel sequences for nonlinear MEMS testing is the subject of future work.

6. Conclusions and further work

This article has presented an evaluation of different IR measurement methods suitable for MEMS BIST. These techniques have been applied to a commercial MEMS accelerometer. As a result, the IRS is the most suitable when even-order nonlinearities exist. We have proved that it has a very high total immunity against even-order nonlinearities. Such nonlinearities vanish for differential systems where the MLS can give the same results as the IRS.

The pseudorandom test method has been modified and applied to a purely nonlinear microbeam with electrothermal excitation. The resulting input/output crosscorrelation samples are the Volterra kernel coefficients needed for modeling, which means that the technique is equally applicable for purely nonlinear MEMS. Finally, the validity of pseudorandom methods for nonlinear circuits has been discussed and work is under way to demonstrate it for a MEMS device.

For the purpose of testing, we will be interested in finding a test signature composed of only several Volterra coefficients that are highly sensitive to faults. A similar signature analysis to that of linear MEMS [14] can be applied. Finally the signature is compared with the tolerance range to decide whether the nonlinear MEMS functions correctly or not.

The MEMS pseudorandom BIST techniques have been modeled and applied to the MEMS accelerometer and the microbeam via Labview and a National Instruments data acquisition card. Work is on the way to fabricate a MEMS device embedding this type of BIST capability.

7. References

[1] S. Sunter and N. Nagi, "Test metrics for analog parametric faults", Proc. of VTS, 1999, pp. 226-234.

[2] H.V. Allen, S.C. Terry, and D.W. de Bruin, "Self-Testable Accelerometer Systems," Proc. of Micro Electro Mechanical Systems, 1989, pp. 113-115.

[3] M. Aikele, K. Bauer,W. Ficker, F. Neubauer, U. Prechtel, J. Schalk, and H. Seidel, "Resonant Accelerometer with Self-test," Sensors and Actuators A, Aug. 2001, vol. 92, no. 1-3, pp. 161-167.

[4] R. Puers and S. Reyntjens, "RASTA–Real-Acceleration-for-Self-Test Accelerometer: A New Concept for Selftesting Accelerometers," Sensors and Actuators A, April 2002, vol. 97-98, pp. 359-368.

[5] L. Zimmermann, J.P. Ebersohl, F. Le Hung, J.P. Berry, F. Baillieu, P. Rey, B. Diem, S. Renard and P. Caillat, "Airbag application: a microsystem including a silicon capacitive accelerometer, CMOS switched capacitor electronics and true self-test capability," Sensors and Actuators A, 1995, vol. A 46, no. 1-3, pp.190-195.

[6] V. Beroulle, Y. Bertrand, L. Latorre, P. Nouet, "Test and Testability of a Monolithic MEMS for Magnetic Field Sensing," Journal of Electronic Testing, Theory and Applications, Oct. 2001, pp. 439-450.

[7] B. Charlot, S. Mir, F. Parrain, and B. Courtois, "Generation of electrically induced stimuli for MEMS self-test", Journal of Electronic Testing: Theory and Applications, Dec. 2001, vol. 17, no. 6, pp. 459-470.

[8] N. Deb and R. D. Blanton, "Built-In Self-Test of CMOS-MEMS Accelerometers," Proc. of International Test Conference, Oct. 2002, pp. 1075-1084.

[9] X. Xiong, Y. L.Wu, andW. B. Jone, "A Dual-Mode Built-In Self-Test Technique for Capacitive MEMS Devices," Proc. of VLSI Test Symposium, April 2004, pp. 148-153.

[10] C. Y. Pan, and K. T. Cheng, "Pseudorandom testing for mixed-signals circuits", IEEE Transactions on Computer-Aided Design of Integrated Circuits and Systems, 1997, vol. 16, no. 10, pp. 1173-1185.

[11] P. S.A. Evans, M. A. Al-Qutayri, and P. R.Shepherd, "A Novel Technique for Testing Mixed-Signal ICs", Proc. of the European Test Conference, 1991, pp. 301-306.

[12] M.Reed and M.Hawksford, "Identification of discrete Volterra series using maximum length sequences", Proc. IEE Circuits, Devices and Systems, 1996, pp. 241-248.

[13] L. Rufer, S. Mir, E. Simeu and C. Domingues, "On-chip pseudorandom MEMS testing", 9th International Mixed-Signal Testing Workshop, 2003, pp. 93-98.

[14] A. Dhayni, S. Mir, and L. Rufer, "MEMS Built-In-Self-Test Using MLS", In Proc. 9th IEEE European Test Symposium, 2004, pp. 66-71.

[15] J. Vanderkooy, "Aspects of MLS measuring systems", presented at the 93rd Convention of Audio Engineering Society, 1992, preprint 3398.

[16] S. Müller, and P. Massarani, "Transfer function measurement with sweeps", Journal of the Audio Engineering Society, 2001, vol. 49, no. 6, pp. 443-471.

[17] A. Farina, "Simultaneous measurement of impulse response and distortion with a swept-sine technique", 108th AES Convention, Journal of the Audio Engineering Society, vol. 48, pp. 350, preprint 5093.

[18] D.D. Rife and J. Vanderkooy, "Transfer Function Measurement with Maximum-Length Sequences", Journal of the Audio Engineering Society, 1989, vol. 37, no. 6.

[19] C. Dunn and M.O. Hawksford, "Distortion Immunity of MLS-Derived Impulse Response Measurements", Journal of the Audio Engineering Society, 1993, vol. 41, no. 5, pp. 314-335.

[20] L. Rolíndez, S. Mir, A. Bounceur and J.L. Carbonero, "A digital BIST for a 16-bit audio $\sum\Delta$ analogue-to-digital converter", 11th IEEE International Mixed-Signals Testing Workshop, 2005, pp. 45-52.